Analysis of nonexponential transient capacitance in silicon diodes heavily doped with platinum

Willie E. Phillips and Jeremiah R. Lowney

Citation: Journal of Applied Physics **54**, 2786 (1983); doi: 10.1063/1.332309
View online: http://dx.doi.org/10.1063/1.332309
View Table of Contents: http://scitation.aip.org/content/aip/journal/jap/54/5?ver=pdfcov
Published by the AIP Publishing

Analysis of nonexponential transient capacitance in silicon diodes heavily doped with platinum

Willie E. Phillips and Jeremiah R. Lowney
Semiconductor Materials & Processes Division, National Bureau of Standards, Washington, D.C. 20234

(Received 4 October 1982; accepted for publication 4 January 1983)

An analysis having improved rigor has been made of the capacitance transient due to thermal emission from charged defect centers in a semiconductor depletion region. This analysis extends the range of applicability of capacitance–transient defect characterization techniques to nonexponential transient conditions which occur in diodes with trap densities of the same order as the net shallow dopant density or in diodes with somewhat smaller trap densities when defect centers are charged initially in only a part of the depletion region. An example of the improvement is shown for three silicon diodes heavily doped with platinum.

PACS numbers: 85.30.De, 71.55.Fr, 72.20.Jv, 85.30.Kk

INTRODUCTION

Defect characterization techniques such as deep-level transient spectroscopy (DLTS)[1] and isothermal transient capacitance (ITCAP)[2] utilize the ability of electrically active defect centers in depletion regions of semiconductors to trap and thermally to reemit charge carriers and thereby to affect the capacitance of the depletion region. It is assumed in conventional DLTS analysis that the measured capacitance transient varies exponentially with time. There are several causes of nonexponential behavior: the emission rate may depend on electric field, spatial nonuniformity of emission or capture rates may exist because of complexing, the density of the deep-level defects may not be small compared to the net shallow dopant density, the junction may not be abrupt, several trapping levels may exist (a sum of exponentials is nonexponential), and trap charging may occur in only part of the depletion region with moderate trap densities (a transient capacitance in series with a constant capacitance). It is the purpose of this paper to use a more rigorous analysis to investigate the capacitance transient in an abrupt-junction, platinum-doped silicon diode which exhibits no electric field or spatial dependencies, but may have: (1) densities of deep levels not small compared to that of shallow levels, or (2) trap charging over only a portion of the depletion layer with moderate trap densities (e.g., as occurs in profiling measurements). The work of Tomokage *et al.*[3] and that of Carcelle *et al.*[4] have considered (1), but not (2).

THEORY OF ANALYSIS

An analysis of a transient which does not exhibit an exponential behavior for either or both of the two reasons listed above can be made in transient capacitance measurements as follows. The transient behavior of the junction capacitance when the trap-filling bias is changed to a larger reverse bias, V_r, is controlled in n-type silicon by the electron emission rate from defect centers. The net time rate of change of n_t, the concentration per unit volume of electrons on the defect centers (i.e., traps) is given by[5]

$$\frac{dn_t}{dt} = e_p p_t - e_n n_t, \tag{1}$$

where e_n is the electron emission rate, e_p is the hole emission rate, and p_t is the concentration of holes on the defect centers. Because the trap must hold either an electron or a hole, the totality condition is satisfied:

$$n_t + p_t = N_t, \tag{2}$$

where N_t is the total defect center density. A differential equation in n_t can be obtained from Eqs. (1) and (2):

$$\frac{dn_t}{dt} + (e_n + e_p)n_t = e_p N_t. \tag{3}$$

The general solution of Eq. (3) is

$$n_t = C_1 \exp[-(e_n + e_p)t] + C_2. \tag{4}$$

The constants C_1 and C_2 can be evaluated at times zero and infinity. At $t = 0$, $n_t = C_1 + C_2 = n_{ti}$ and at $t = \infty$, $n_t = C_2 = n_{tf}$. Equation (4) can be written

$$n_t = n_{tf} + (n_{ti} - n_{tf})\exp[-(e_n + e_p)t]. \tag{5}$$

Under ideal one-sided step-junction conditions, the junction capacitance C at reverse bias V_r is[6]

$$C^{-2} = C_b^{-2} + \frac{2(V_r - V_c)}{q\epsilon A^2(N_d - n_t)}, \tag{6}$$

where C_b is the junction capacitance at some reduced trap-filling bias, V_c, A is the junction area, ϵ is the absolute dielectric constant (permittivity) of silicon, N_d is the shallow dopant density (assumed to be spatially uniform), and q is the electronic charge. (Note: SI units are used throughout this paper.) This equation is valid only if there is no significant compensation of the shallow dopants by the traps as discussed by Sah and Reddi.[7] The results of an extension of their theory for the present cases is given in the Appendix and a more general expression leading to a modification of Eq. (6) is obtained. The result of this analysis has shown that for sufficiently large reverse biases, there are ranges of bias voltages and times for which Eq. (6) is valid if the factor 2 is replaced by a dimensionless factor α which is constant during each menasurement but changes in value with experimental conditions.

This generalization of Eq. (6) can be solved for n_t to give

$$n_t = N_d - \frac{\alpha(V_r - V_c)C_b^2 C^2}{q\epsilon A^2(C_b^2 - C^2)}. \quad (7)$$

At the initial time ($t = 0$), the reverse bias is reapplied (at the end of the trap-filling period), n_t is n_{ti}, and C is C_i. In the infinite time limit or final steady-state condition n_t is n_{tf} and C is C_f. Substitution of n_t, n_{ti}, and n_{tf} into Eq. (5) and solution for the exponential term gives:

$$\exp[-(e_n + e_p)t] = \frac{(C_b^2 - C_i^2)(C_f^2 - C^2)}{(C_b^2 - C^2)(C_f^2 - C_i^2)} \equiv C_r. \quad (8)$$

The right side of Eq. (8) is a capacitance ratio and will be called C_r. The same equation can also be expressed in terms of C as:

$$\frac{C^2}{C_b^2 - C^2} = \frac{C_f^2}{C_b^2 - C_f^2} + \left(\frac{C_i^2}{C_b^2 - C_i^2} - \frac{C_f^2}{C_b^2 - C_f^2}\right) e^{-t/\tau}, \quad (9)$$

where $\tau = 1/(e_n + e_p)$.

For the special case where the trap density is small compared to the shallow dopant density (i.e., $N_t/N_d \ll 1$), Eq. (9) reduces to the customary exponential form for sufficiently large C_b. Since C is bracketed by C_i and C_f, all the denominators in Eq. (9) will be approximately equal if $C_b^2 - C_f^2 \approx C_b^2 - C_i^2$. When $N_t/N_d \ll 1$ and C_b sufficiently large for exponentiality, $(C_f^2 - C_i^2)/C_f^2 = N_t/N_d$. Therefore, one obtains $C_b^2 - C_f^2 \approx C_b^2 - C_f^2\,(1 - N_t/N_d)$. This expression shows that in the limit of very low trap density ($N_t/N_d \to 0$), the denominators are nearly equal for all $C_b > C_f$. For more moderate trap densities, however, C_b must be sufficiently larger than C_f such that $(C_b^2 - C_f^2)/C_f^2 \gg N_t/N_d$. When the denominators in Eq. (9) are approximately equal,

$$C^2 - C_f^2 \simeq (C_i^2 - C_f^2)e^{-t/\tau}.$$

The difference of squares can be factored and for $C_i \approx C_f \approx C$, the sums $(C + C_f)$ and $(C_i + C_f)$ are approximately $2C_f$ so that

$$C \simeq C_f + (C_i - C_f)e^{-t/\tau}. \quad (10)$$

Therefore, the conventional analysis in which this exponential transient is assumed is valid for N_t/N_d small and for C_b sufficiently large. Under such conditions, a plot of $\log[(C - C_f)/(C_i - C_f)] \equiv \log C_n$ against time would be linear with a slope proportional to $1/\tau$. However, when these conditions are violated, as is shown below in the devices studied here, it is necessary to use the more rigorous analysis leading to Eq. (8) which predicts that a plot of $\log C_r$ against time would be linear with a slope proportional to $-1/\tau$ (equal to $-1/\tau$ if the natural logarithm is used).

DEVICE FABRICATION

The three devices used in this study are gated p^+n and n^+p diodes (device No. 10 of test pattern NBS-3)[8] and were fabricated on 3- to 5-Ω cm ⟨111⟩ n- or p-type silicon wafers. Boron predeposition and diffusion through 0.432-mm diameter openings in 500-nm of field oxide formed a 450-nm deep p^+n junction. The back side of this device was stripped and coated with a spun-on platinum emulsion followed by a drive-in at 850 °C for 2 h in a dry nitrogen ambient for device No. 1, and at 900 °C for 1 h for device No. 2. The residual platinum was etched from the back side. Contact opening, top metallization (aluminum), back metallization (gold plus 0.6% antimony), top metal definition, and a 10-min 500 °C microalloy in dry nitrogen completed the fabrication of the structure. The structure was hermetically packaged in a TO-100 header on a ceramic chip close to an electrically isolated temperature-sensing diode which was in good thermal contact with the test device because of high thermal conductivity of the ceramic. The n^+p diode (device No. 3) was fabricated in a complementary manner with boron replaced by phosphorus and with a platinum diffusion temperature of 1000 °C for 1 h.

DEVICE CHARACTERISTICS

The abruptness of the device junctions was tested; a plot of C^{-2} against V was found to be linear at room temperature and to obey the ideal diode equation, Eq. (6). The shallow dopant density N_d on the lightly doped side was calculated from these data. At the temperatures of the measurements (80–120 K), however, the C^{-2} versus V plots were nonideal as shown in Fig. 1. The theoretical curves (shown as solid lines) given by Eq. (A5) in the Appendix give a reasonable fit to the data (shown as circles) for devices No. 1 and 2. The

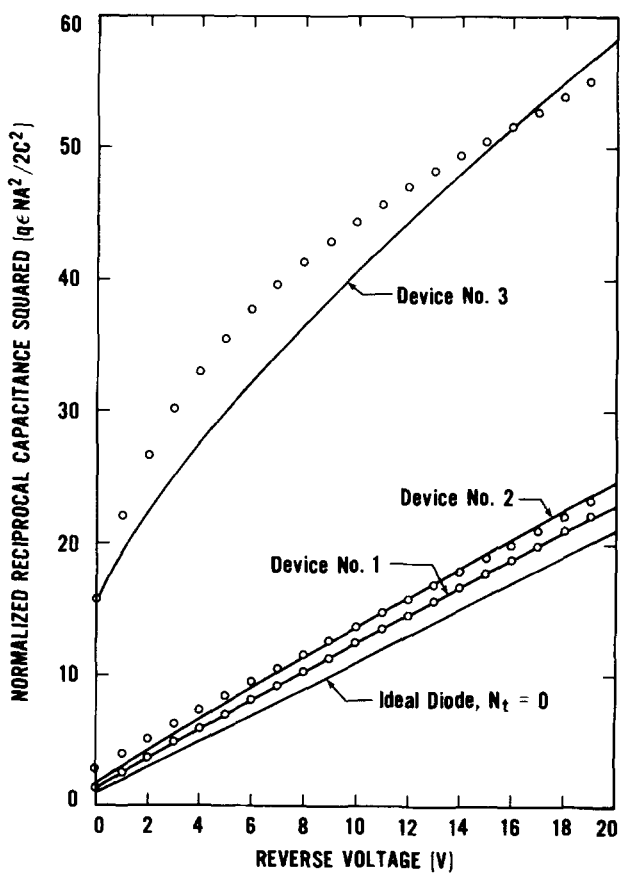

FIG. 1. Normalized C^{-2} vs V plots of experimental data on moderately, heavily, and very heavily platinum-doped silicon diodes at low temperatures (devices No. 1–3, respectively). The solid lines are theoretical curves based on the present model, Eq. (A5), for these three devices and for an ideal diode.

trap and ionized dopant densities of Eq. (A5) N_T and N_d^+ were chosen to give a good fit both to these sets of data and to the transient capacitance data. The density ratios used for device No. 1 were $N_t/N_d = 0.19$ and $N_d^+/N_d = 0.78$ with a dopant density (donors) of $N_d = 1.08\times10^{15}$ cm^{-3}. The ratios for device No. 2 were $N_t/N_d = 0.38$ and $N_d^+/N_d = 0.77$ with $N_d = 1.21\times10^{15}$ cm^{-3}. In device No. 3, the dopant density (acceptors) was $N_a = 3.01\times10^{15}$ cm^{-3} and the density ratios were $N_t/N_a = 0.90$ and $N_a^-/N_a = 0.925$. The discrepancy between the model and the experimental data increases with increasing platinum density and is significant for device No. 3. It is not certain whether this discrepancy results from an inadequacy of the theory or from an inhomogeneity of trap density in the specimen near the junction.

The spatial dependence of the emission rate was investigated in device No. 2 by ITCAP measurements in incremental depletion layers of uniform width and electric field distributions. These test were accomplished by (1) applying a reverse bias of 2 V to the specimen diode, (2) waiting for equilibrium conditions, (3) partially collapsing the depletion region by reducing the bias to 0 V, (4) waiting a few seconds for the traps in the previously depleted region to fill with majority carriers, and (5) then restoring the depletion bias to 2 V. The capacitance transient response was recorded on an x–y recorder during and following these bias changes (see Fig. 2). The transient response was analyzed to obtain the emission rate. The measurements were repeated at a greater average distance from the junction by increasing the initial value of depletion bias to values greater than 2 V, but maintaining the same width of the active region (i.e., the portion of the space-charge region which upon reduction of the bias fills with majority carriers). Because the C^{-2} versus V plot was linear, an abrupt junction was assumed in which the total depletion depth varies as the square root of the voltage across the depletion layer. Thus the bias voltage during the trap-filling time V_c and the bias voltage during the time of observing the emission transient V_r can be selected so that the width of the active region is constant but is located at various distances from the junction. The voltage across this active portion of the depletion region was held constant as V_r and V_c (and thus the depth) were changed. The series of such measurements gave transients with a constant emission rate in the range of V_r of 2–20 V reverse bias. The tests were repeated with a larger average electric field (minimum $V_r = 5$ V) with the same resultant constant emission rate. A completely independent experiment with sulfur-doped silicon showed variations with both electric field and position of the active region. Therefore, for the case of this platinum-doped device, it was concluded that the emission rate is independent both of these electric field variations in the depletion region and of the position of the active region relative to the junction at distances greater than the zero-bias depletion depth.

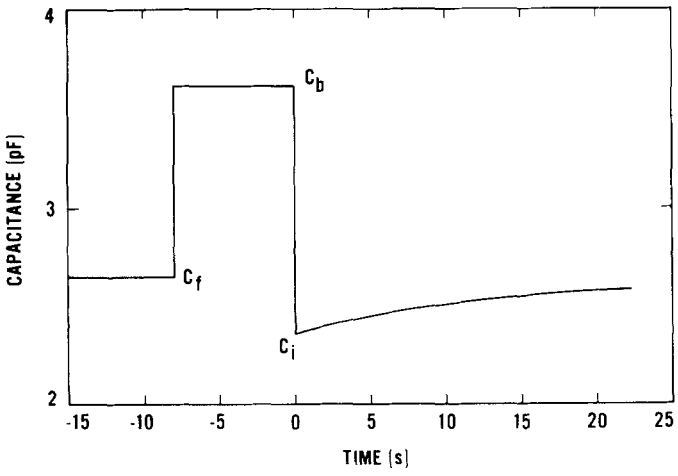

FIG. 2. Transient capacitance response against time of a p^+n silicon diode (device No. 2) heavily doped with platinum ($N_t/N_d \approx 0.38$). Initial reverse bias is 20 V, charging reverse bias is 9.35 V, and the temperature is 87.7 K. $C_i = 2.36$ pF, $C_f = 2.65$ pF, and $C_b = 3.62$ pF.

RESULTS

A typical as-measured isothermal capacitance variation is shown in Fig. 2. The absence of a transient in C_b (the capacitance under trap-charging bias conditions) indicates that a slow-capture region resulting from spatially nonuniform capture rates[9,10] is not a problem for device No. 2. The same is true for device No. 1. A short transient is observed on device No. 3. When a transient is observed, one can wait until the traps in the slow-capture region are filled (as was done for device No. 3).

In Fig. 3, the transient response of Fig. 2 has been replotted (shown as circles) from digitized data as the conventional DLTS curve of log C_n against time. The plot is seen to be slightly nonlinear indicating that the measured capacitance transient is nonexponential. The instantaneous time constant (reciprocal of the emission rate) is proportional to the slope of the data and is dependent upon the time at which it is measured. The initial slope (shown as a dashed line) has a time constant of 12.7 sec. The nonexponentially of the capacitance transient is attributed to violation of the small N_t/N_d approximation (here $N_t/N_d = 0.38$) and to charging of traps in only part ($\sim 1/3$) of the depletion region. In contrast, a plot of the logarithm of C_r of Eq. (8) against time for the transient of Fig. 2 is shown as solid dots in Fig. 3. The solid line is a weighted linear regression fit to the data with a weighting factor of C_r and shows that these data are linear to within experimental error. The + 's are obtained from Eq. (A1) and are in good agreement with the experimental data. This agreement serves to justify the application of the present model to devices of this kind.

The capacitance ratios of a less heavily doped ($N_t/N_d = 0.19$) diode (device No. 1) are shown in Fig. 4. Again, the solid circles are log C_r, the open circles are log C_n, and the + 's are theoretical values of the same quantities as calculated by Eq. (A1). The linearity of the C_r values and the good agreement between the model presented in the Appendix and the experimental data are again obtained.

A more dramatic case is shown in Fig. 5 for the more heavily doped n^+p diode (device No. 3, $N_t/N_a = 0.90$) for two bias sequences. One curve shows data (circles) and the-

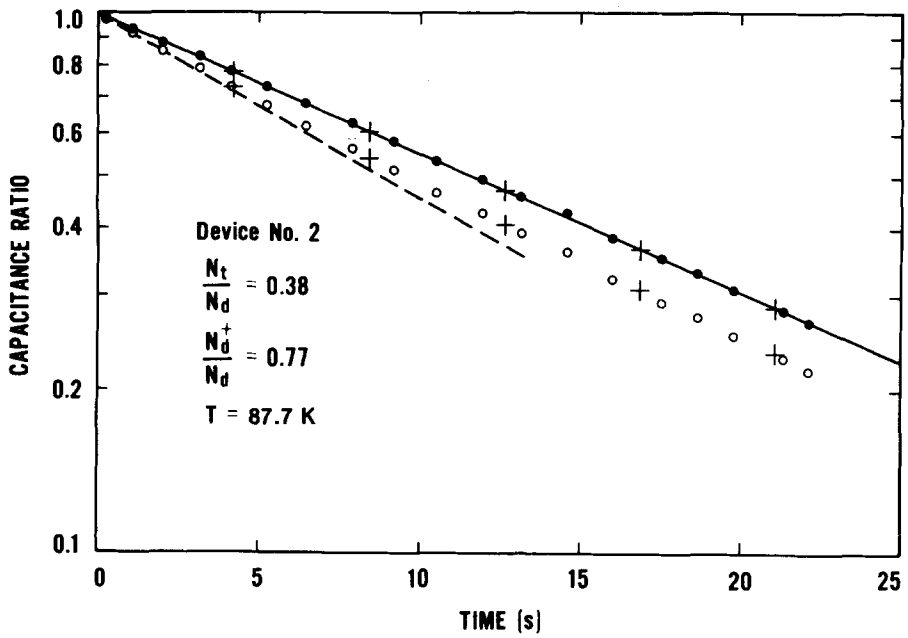

FIG. 3. Semilogarithmic digitized and normalized plot of the transient capacitance ratio C_n for the data of Fig. 2 (shown as open circles) against time. The dashed line is the initial slope. The solid circles represent the same data with the present more rigorous analysis which leads to the capacitance ratio C_r given by Eq. (8). The solid line is a weighted linear regression fit to the data of log C_r against time. The + 's are theoretical values calculated by use of Eq. (A1) with $C_i = 2.36$ pF, $C_f = 2.65$ pF, and $c_b = 3.62$ eV.

ory (×'s) for a trap-filling bias of 4 V, and the other shows data (squares) and theory (+ 's) for a trap-filling bias of 6 V. The bias during the emission transient for each is 9 V. The slight difference in the solid weighted linear regression lines through the C_r data is attributed to a systematic temperature difference of about 0.05 K between these runs. The solid circles and squares which correspond to log C_r at the beginning of the transient are below the fitted line as predicted by calculations from Eq. (A1). For this reason, experimental points before the time $\tau/2$ are excluded from the linear regression fit but are shown in Fig. 5. Even though the theory is less successful in predicting log C_n for this case, the agreement is very good for log C_r.

The significance of the linearity of the log C_r plots in Figs. 3, 4, and 5 is that the present analysis correctly accounts for the large trap density which leads to compensation of the partially deionized dopants, and for the unchanging capacitance in the part of the depletion region in which the traps are never charged. In Fig. 3, the time constant was found to be 16.88 ± 0.03 s, which is about 34% greater than the time constant indicated by the initial slope of the uncorrected capacitance data and about 16% greater than that of a straight line fitted to all of the uncorrected data. The above uncertainty value of ± 0.03 s is the one standard deviation uncertainty in the statistical fit only and does not include any instrumentation error. In Fig. 4, the time constant for the linear regression line is 13.92 ± 0.03 s which is 5% more than the uncorrected value obtained from a linear regression line fitted to the open circles. In Fig. 5, the time constant for the 9, 6, 9 V bias sequence (solid squares) is 70.20 ± 0.05 s,

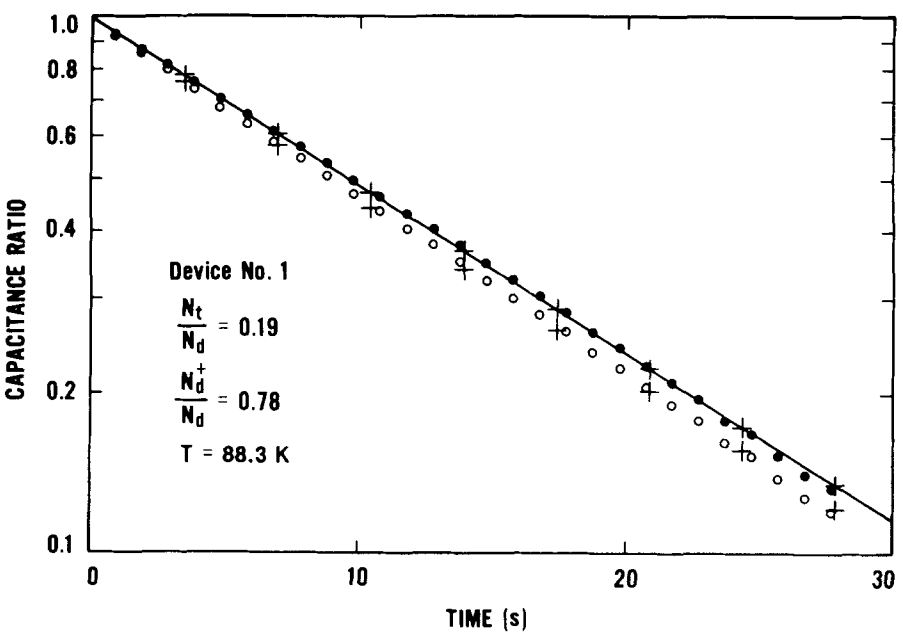

FIG. 4. Semilogarithmic digitized and normalized plot of the transient capacitance ratio C_n (shown as open circles) and C_r (shown as solid circles) against time for a p^+n silicon diode (device No. 1) moderately doped with platinum ($N_t/N_d = 0.19$). The solid line is a weighted linear regression fit to the data of log C_r against time. The + 's are theoretical values calculated by use of Eq. (A1) with $C_i = 4.55$ pF, $C_f = 4.72$ pF, and $C_b = 6.05$ pF as deduced by curve fitting. Experimental values for this capacitance transient are $C_i = 4.56$ pF, $C_f = 4.72$ pF, and $C_b = 6.03$ pF. Initial reverse bias is 5 V, charging bias is 2.5 V, and the temperature is 88.3 K.

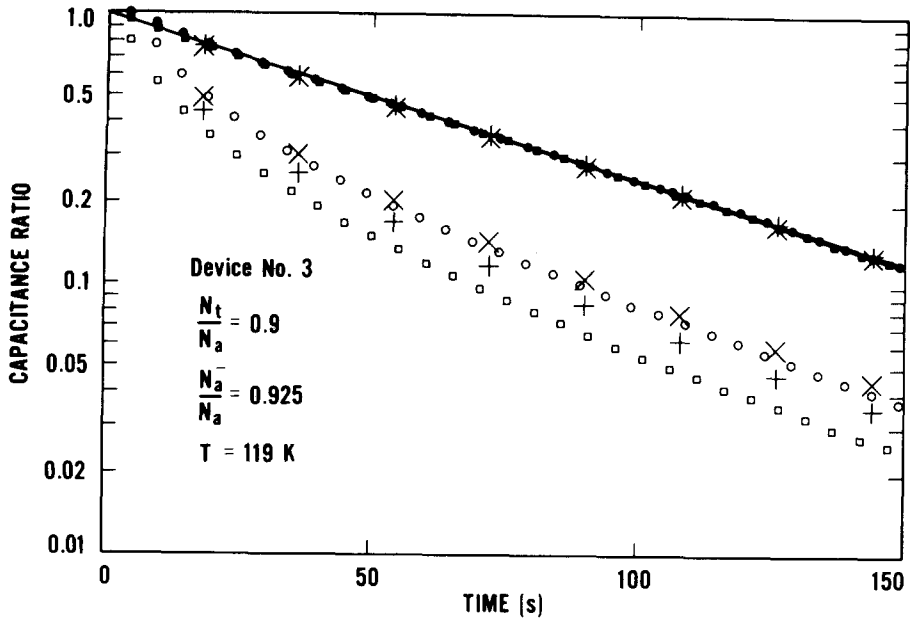

FIG. 5. Semilogarithmic digitized and normalized plot of the transient capacitance ratios C_n (shown as open circles and squares) and C_r (shown as solid circles and squares) against time for a n^+p silicon diode (device No. 3) very heavily doped with platinum ($N_t/N_a = 0.9$). Initial reverse bias is 9 V, charging reverse bias is 6 V for the squares and 4 V for the circles, and the temperature is 119 K. Measured capacitance for the squares are $C_i = 2.20$ pF, $C_f = 3.17$ pF, and $C_b = 3.39$ pF and for the circles are $C_i = 2.03$ pF, $C_f = 3.17$ pF, and $C_b = 3.62$ pF. The + 's are theoretical values for the 9, 6, 9 V biasing sequence ($C_i = 2.36$ pF, $C_f = 3.34$ pF, and $C_b = 3.65$ pF), and the × 's are theoretical values for the 9, 4, 9 V biasing sequence ($C_i = 2.07$ pF, $C_f = 3.34$ pF, and $C_b = 3.94$ pF). The solid lines are linear regression fits to the two sets of data with points prior to $t = 35$ sec excluded.

which is about 4.5 times greater than the time constant indicated by the initial slope of the uncorrected capacitance data (open squares).

The time constants reported here for platinum in n-type silicon are in good agreement with an extrapolation of previous characterization measurements on devices similar to device No. 1.[11] Previous measurements on the p-type diodes[11] were made on heavily platinum-doped devices with biases in the nonlinear region of the C^{-2} versus V curve and give an extrapolated time constant less than the time constant reported here.

CONCLUSIONS

It is concluded that the use of the present more rigorous analysis can correct for the nonexponentiality introduced by a large density of defect centers which compensate the partially deionized shallow dopants at low temperature. It also corrects for trap charging in only a part of the depletion region at moderate levels of defect density. It was shown that the conventional exponential approximation is adequate only for small trap densities and that the correction for charging of these traps in only part of the depletion region decreases with decreasing trap density. The present analysis extends the range of applicability of transient capacitance techniques to conditions encountered in practical devices (e.g., N_t/N_d not $\ll 1$) and in more detailed measurements (e.g., deep level profiling).

ACKNOWLEDGMENT

This work was conducted as part of the Semiconductor Technology Program at NBS and was supported by the Division of Electric Energy Systems, Department of Energy (Task Order A021-EES).

APPENDIX

At low temperatures, the Fermi level lies close to the conduction band edge in n-type silicon or to the valence band edge in p-type silicon. If platinum is present, the Fermi level lies below the platinum donor level in p-type material or above the platinum acceptor level in n-type material. These levels then become charged and the platinum tends to compensate the shallow dopant. At sufficiently low temperatures significant compensation can occur in heavily Pt-doped diodes because the shallow dopants deionize. The result is that a p–n junction diode heavily doped with platinum has a C^{-2} versus V relationship which is nonlinear at low temperatures.

In order to model this situation, the theories of Sah and Reddi[7] and of Tomokage *et al.*[3] have been extended to include effects due to incomplete collapse of the space charge region and to compensation of the shallow dopant. Consider the space-charge region of a p^+n or an n^+p diode to be divided into three regions. The part of the space-charge region on the heavily doped side of the junction is neglected as in the previous work.[7,3] The effect of the platinum acceptor in p-type material or the platinum donor in n-type material is ignored as in the previous work[7,3] as well. For a p^+n diode the first region, nearest the metallurgical junction on the lightly doped n-type side, is taken to have a fixed bulk charge density of qN_d, where N_d is the shallow donor density. The extent of this region is determined by the crossing of the majority carrier quasi-Fermi level and the platinum donor level in p-type material or the platinum acceptor level in n-type material when the bias voltage is V_c, during the trap filling period.

The second region is taken to have a time-varying bulk charge density of $q(N_d - n_t)$ where n_t is the occupied trap density. The extent of this region is between the end of the first region and the crossing of the same quasi-Fermi level and platinum level when the bias voltage is V_r, the maximum reverse bias during which the transient emission is observed. The third region extends from the end of the second region and has a fixed bulk charge density of $q(N_d^+ - N_t)$ where N_d^+ is the average density of ionized donors and N_t is the

total trap density (i.e., all the traps are occupied and contribute to compensation). Since the quasi-Fermi level is close to the band edge in this region, there is some freezeout of the shallow dopant so that N_d^+ is less than N_d. The extent of this region is determined by the total width of the space charge region as found by integrating Poisson's equation twice. Since considerable compensation can occur between the filled traps and the ionized shallow dopants, this third region can be very wide. The result is a significant decrease in the junction capacitance, which is given by $\epsilon A/w(t)$ at high frequencies relative to trap emission rate, where $w(t)$ is the width of the space-charge region and A is the junction area.

The result of this extension of the Sah–Reddi model[7] is that the high frequency capacitance $C(t,V)$ is given by

$$C^{-1}(t,V_r)=\left(\frac{2}{q\epsilon A^2 N_d^+}\right)^{1/2}\frac{1}{(N_d-n_t)} \times\{\beta\gamma+[\beta^2\gamma^2+N_d^+(N_d-n_t) \times(V_r+V_d-V_\alpha-\beta\gamma^2/N_d^+)]^{1/2}\}, \quad \text{(A1)}$$

where

$$\beta=N_T-n_t+N_d-N_d^+ \quad \text{(A2)}$$

and

$$\gamma=\left[\frac{N_d^+\,\phi}{N_d^+-N_T}\right]^{1/2}. \quad \text{(A3)}$$

The built-in diffusion potential V_d is taken to be approximately 1 V, i.e., slightly less than the energy gap. The potential ϕ is the difference between the energy of the quasi-Fermi level and the trap level. This quantity is always greater than or equal to zero; if it were less than zero, the traps would be empty and their effect would disappear. The platinum donor level is approximately 320 meV[12] above the valence band, and the platinum acceptor level is approximately 230 meV below the conduction band.[12] The corresponding values for ϕ are approximately 250 meV in p-type material and 160 meV in n-type from estimates of the Fermi energy in material containing $\sim 10^{15}$ cm^{-3} shallow dopants at ~ 100 K.

The voltage V_α is given by

$$V_\alpha=(q/2\epsilon)n_t\left[\epsilon A C^{-1}(\infty,V_c)-\left(\frac{2\epsilon\,\phi}{q(N_d^+-N_T)}\right)^{1/2}\right]^2, \quad \text{(A4)}$$

where

$$C^{-1}(\infty,V)=\left(\frac{2}{q\epsilon A^2 N_d^+}\right)^{1/2}\{\rho\gamma+[\rho^2\gamma^2+(N_d^+/N_d) \times(V+V_d-\rho\gamma^2 N_d/N_d^+)]^{1/2}\} \quad \text{(A5)}$$

and

$$\rho=(N_T+N_d-N_d^+)/N_d. \quad \text{(A6)}$$

In Eq. (A1) it is assumed that

$$n_t=N_T e^{-t/\tau}, \quad \text{(A7)}$$

which should be true at the low temperatures at which the measurements were made. Equations (A1)–(A7) are written for shallow donors and deep acceptor traps, but analogous equations exist for shallow acceptors and deep donor traps.

The values for the trap densities and ionized shallow dopant densities were obtained by fitting approximately both the C^{-2} versus V data and the total change in capacitance during the transient. The total shallow dopant density was obtained from room temperature C^{-2} versus V plots, which obeyed the ideal linear relationship for an abrupt junction. The amount of deionization found from these analyses was considered very reasonable when compared with calculations of the neutrality condition at these temperatures for samples containing no traps.

A comparison of Eq. (A1) and Eq. (6) shows that they are in agreement only if $\gamma=0$, i.e., $\phi=0$. However, if the reverse bias voltages V_c and V_r are sufficiently large and sufficiently close to each other, the effect of $\gamma>0$ is to alter Eq. (6) such that for sufficiently long times, the form of Eq. (6) remains valid except that the factor 2 must be replaced by a dimensionless constant α which is in general greater than 2. This approximation is given by Eq. (7). The validity of this approximation is shown by the result of fitting the capacitance ratio C_r, given by Eq.(8), which is discussed in the *Results* section. The dependence of α on bias voltages and time is very complex, and it is better to use the fundamental Eq. (A1) to determine the validity of the approximation given by Eq. (7).

[1] D. V. Lang, J. Appl. Phys. **45**, 3023 (1974).
[2] W. E. Phillips and M. G. Buehler, in *Semiconductor Measurement Technology: Progress Report*, July 1 to September 30, 1976, edited by W. M. Bullis and J. F. Mayo-Wells, NBS Special Publication 400-36 (U.S. GPO, Washington, D.C., 1978), pp. 20–22.
[3] H. Tomokage, H. Nakashima, and K. Hashimoto, Jpn. J. Appl. Phys. **21**, 67 (1982).
[4] J. E. Carcelle, P. Cartujo, J. R. Morante, J. Barbolla, J. C. Brabant, and M. Brousseau, Rev. Phys. Appl. **15**, 843 (1980).
[5] M. G. Buehler, Solid-State Electron. **15**, 69 (1972).
[6] W. Shockley, Bell Sys. Tech. J. **28**, 435 (1949).
[7] C. T. Sah and V. G. K. Reddi, IEEE Trans. Electron Devices **ED-11**, 345 (1964).
[8] M. G. Buehler, *Semiconductor Measurement Technology: Microelectronic Test Pattern NBS-3 for Evaluating the Resisitivity–Dopant Density Relationship of Silicon*, NBS Special Publication 400-22 (U.S. GPO, Washington, D.C., 1976).
[9] H. G. Grimmeiss, L. A. Ledebo, and E. Meijer, Appl. Phys. Lett. **36**, 307 (1980).
[10] J. A. Borsuk and R. M. Swanson, J. Appl. Phys. **52**, 6704 (1981).
[11] F. F. Oettinger and R. D. Larrabee, editors, *Measurement Techniques for High Power Semiconductor Materials and Devices: Annual Report, October 1, 1978 to September 30, 1979*, Interagency Report NBSIR 80-2061 (U.S. GPO., Washington, D.C., 1980), pp. 16–17.
[12] S. D. Brotherton, P. Bradley, and J. Bicknell, J. Appl. Phys. **50**, 3396 (1979).